

Project 1

Andrew Dowling

October 3, 2023

Abstract

This project details the numerical solution of the Bessel differential equation and the numerical solution to a Gaussian integral. The Bessel equation solution was approximated with both Euler's Method and 4th order Runge-Kutta. Both numerical solutions are compared to a significantly high amount of terms from the open form solution Bessel Functions given by the Frobenius method. The Gaussian integral solution is determined using Reimman sums, a trapezoidal sum, and a Simpson's rule. These solutions are compared to similar solution methods implimented by Scipy.

1 Bessel Equation

1.1 Background

The Bessel Equation is a second order ODE of the following form.

$$x^2 \frac{d^2 y}{dx^2} + x \frac{dy}{dx} + (x^2 - n^2)y = 0 \quad (1)$$

For the purposes of finding a numeric solution, it can be rewritten

$$\frac{d^2 y}{dx^2} = -\frac{1}{x} \frac{dy}{dx} - \frac{(x^2 - n^2)}{x^2} y \quad (2)$$

which in turn can be transformed into a series of first order ODE's.

$$\frac{dz_1}{dx} = z_2 \quad (3)$$

$$\frac{dz_2}{dx} = -\frac{1}{x} z_2 - \frac{x^2 - n^2}{x^2} z_1 \quad (4)$$

The Bessel Equation does not have a closed form analytic solution however, for the purposes of this assignment it was hopeful a sufficiently high number of terms from the Frobenius method solution (of the Bessel function of the first kind) could play the role of the analytic solution. 50 terms were kept in the Frobenius method solution and all ranges of the Bessel equation solutions will be kept to at most (0, 25)

$$J_n = \sum_{l=0}^{\infty} \frac{(-1)^l}{2^{2l+n} l! (l+n)!} x^{2l+n} \quad (5)$$

1.2 Phenomena to verify

There are two properties of Bessel functions to be verified are given by the following equations.

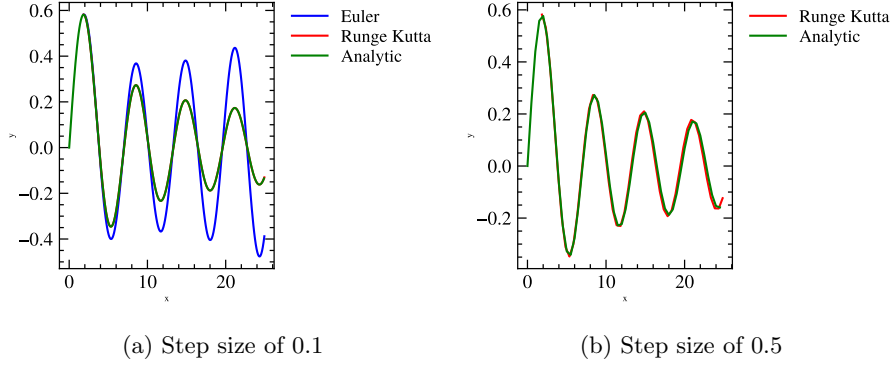
$$J_{-n} = (-1)^n J_n \quad (6)$$

$$\frac{d}{dx} J_n = \frac{1}{2} (J_{n-1} - J_{n+1}) \quad (7)$$

1.3 Results

Given the form of equation 2 and 4, $x = 0$ is not a useable starting point for either the 4th order Runge Kutta method or the Euler method. This complicates things as now boundary conditions must be chose at $x \neq 0$. To ensure that only the bessel function of the first kind is represented, boundary conditions for order $n = 1$ are chosen as $y(1.8412) = 0.5819$ and $\left. \frac{dy}{dx} \right|_{1.8412} = 0$. Similar conditions are chosen for the $n = 2$ case so that the starting place of the curve is where the derivative is 0.

It can be seen that the 4th order Runge Kutta method is vastly superior to the Euler method. While both the 4th order Runge Kutta and analytic solutions are curves similar to that of a decaying sin function, the Euler solution starts to decay, yet actually begins to increase at larger x. Even with a larger step size, the Runge Kutta outperforms the Euler method.



1.3.1 Phenomena 1

The Runge Kutta method was used to verify a specific example of eqn 6.

$$J_{-1} = -J_1 \quad (8)$$

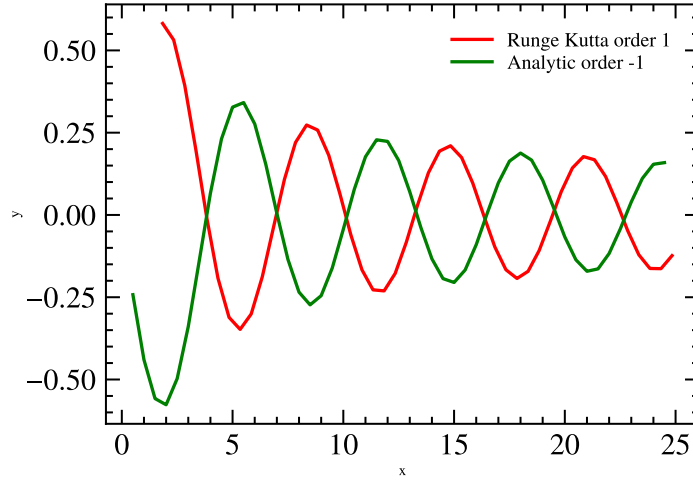


Figure 2: Comparison of the 4th order Runge Kutta solution of a 1st order Bessel Function with the analytic solution to a Bessel Function of order -1

1.3.2 Phenomena 2

The Runge Kutta method was used to verify a specific example of eqn 7. Here, the derivative of the solution is needed, and so the method of breaking the Bessel Equation into a series of first order ODE's becomes more useful.

$$\frac{d}{dx} J_2 = \frac{1}{2}(J_1 - J_3) \quad (9)$$

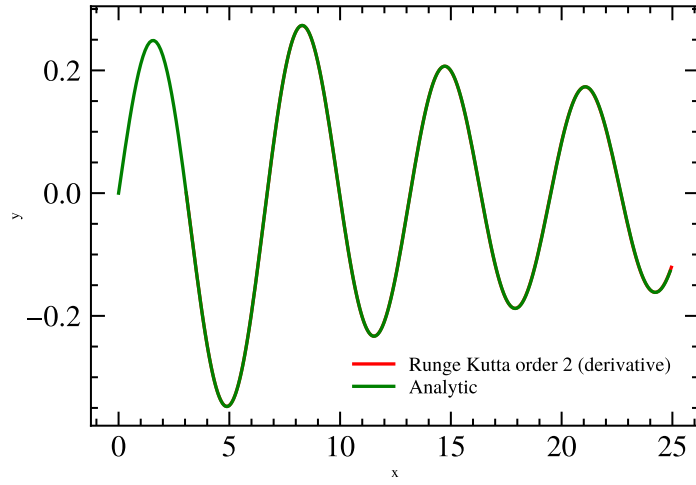


Figure 3: Comparison of the derivative 4th order Runge Kutta solution to a second order Bessel equation with its equivalent analytic comparison

2 Gaussian Integral

2.1 Physical Background

Countless physical distributions can be well approximated by a Gaussian distribution. Currently, I'm looking into the time resolution of an Analog to Digital converter that would potentially be used in an upcoming upgrade of part LHCb detector at Cern. When a charged particle interacts with a sensor, an analog pulse is emitted from the sensor. This pulse is amplified and subsequently digitized by the ADC. The ADC associates a time value to each position on the pulse relative to the beginning of some clock cycle. This information can be used to timestamp the particle, and potentially associate time-of-flight information to that particle. IE, if the time at interaction is also known, the difference between time and the time in which the particle interacted with the sensor would be the time-of-flight for that particle.

As the ADC is taking a continuous pulse and measuring it discretely, the accuracy of the timestamp associated with the particle is limited. An experiment I did over the summer measured this inaccuracy. By repeatedly sending two identical pulses separated by a fixed time interval (using cable length) to one channel on the ADC, the time resolution can be determined by analyzing the distribution of the differences between the timestamps of the two pulses.

The AARDVARC ADC chip has a measured time resolution of 10ps. Suppose a student sends a laser pulses at 40MHz to a sensor that reads into the chip, and the chip is synchronized with a 40MHz clock such that analog pulses always arrive at the ADC a fixed time after the time to digital records $t = 0$. If 10,000 laser pulses are emitted in total, how many will be recorded as arriving 5ps later than they did in reality?

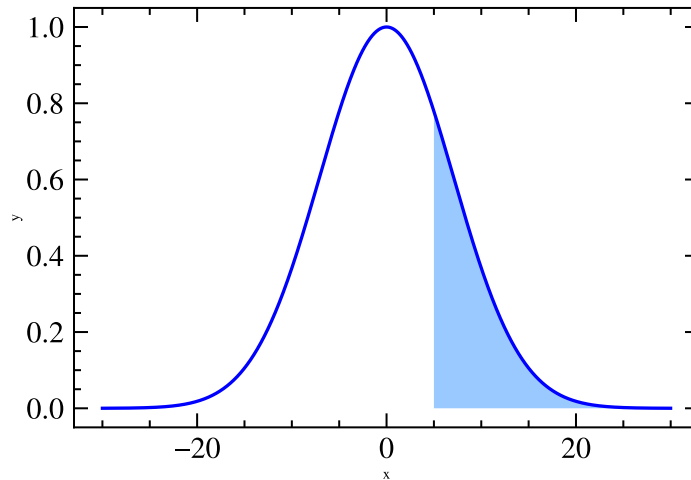
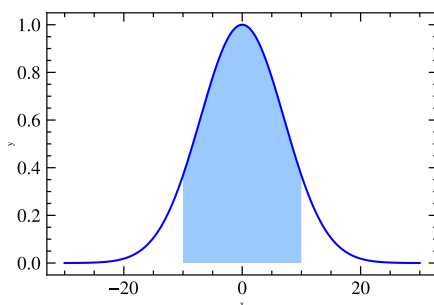


Figure 4: Integral needed to calculate for physics question posed

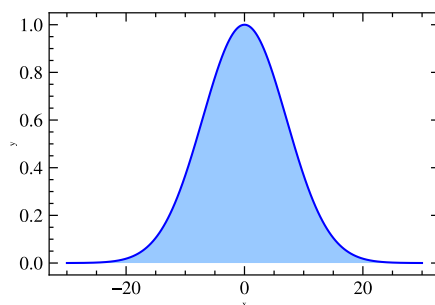
2.2 Other Phenomena to Verify

To verify that the integration methods attempted are correct, two phenomena of integrals similar to the problem described will be proven. The first being that 68.27% of the data described by a Gaussian distribution will be within one standard deviation of the mean. The second being the known value of a Gaussian integral over the range $(-\infty, \infty)$.

$$\int_{-\infty}^{\infty} \exp\left(-\frac{x^2}{2\sigma^2}\right) = \sqrt{2\pi} \quad (10)$$



(a) First phenomena to verify



(b) Second phenomena to verify

2.3 Results

A Reimman sum uses the volume of rectangles to approximate the integral of a function. The height of each rectangle is determined by the value of the function at either the left, right, or middle of the rectangles width. The resultant area is more accurate when more rectangles are used, however, required computational power also increases with the amount of rectangles.

A trapezoidal sum uses volumes of trapezoids to better approximate the integral of a function. The height of each side of the trapezoid is determined by the value of the function at that side of the trapezoid. Similiar to the Reimman sum, the resultant area is more accurate when more trapezoids are used, however, required computational power also increases with the amount of trapezoids.

Simpson's Method goes one step further in approximating the integral by using a polynomial function to describe the behavior of the curve at discrete points. Like both the Reimman sum and trapezoidal sum, the resultant area is more accurate when more points are used, however, required computational power also increases with the amount of trapezoids.

2.3.1 Phenomena 2

Since it will be needed in the next two sections, the Gaussian integral with the bounds $(-\infty, \infty)$ should be found first. Of course, we cannot numerically integrate from $(-\infty, \infty)$, so a bounds of $(-10, 10)$ is chosen as $10 \gg \sigma$. In fact, choosing significantly higher bounds for this integral causes issue; python will give larger areas for high values of $|x|$ than expected. It is suspected that this is due issues when subtracting very small numbers as seen on the tail ends of the Gaussian distribution.

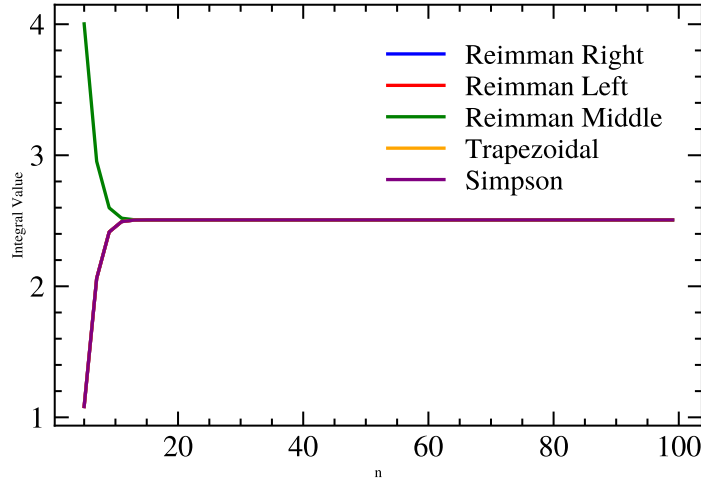


Figure 6: Value of integral for various number of points used in integral calculation

When reasonable bounds are used $((-10, 10))$, an agreement of greater than 99.98% with the expected value of $\sqrt{2\pi}$ is found using any of the mentioned methods. Unsurprisingly, the volume calculated from a right-hand Reimman sum is exactly the same as the volume calculated from a left-hand Reimman sum due to symmetry.

2.3.2 Phenomena 1

Section 2.3.1 is a specific case ($\sigma = 1$) of the normalized Gaussian distribution.

$$\frac{1}{\sqrt{2\pi}} \exp\left(-\frac{1}{2} \frac{x^2}{\sigma^2}\right) \quad (11)$$

To verify phenomena 1, we can again choose $\sigma = 1$ to evaluate the following integral.

$$V = \frac{1}{\sqrt{2\pi}} \int_{-1}^1 \exp\left(\frac{-x^2}{2}\right) \quad (12)$$

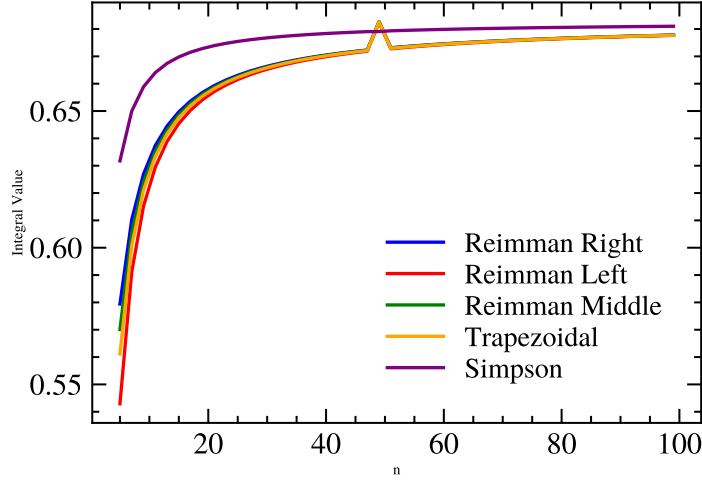


Figure 7: Value of integral for various number of points used in integral calculation, an unexplained bump in the value occurs for all methods at $n = 50$ with the exception of the Simpson method.

All methods converge to an agreement of 68.27% when sufficient points are used. However, there is a strange bump in the value when a specific amount (50) of points are used for some unknown reason.

2.3.3 Physics Problem

Now the pieces are in place to tackle the physics problem proposed. The following integral should be calculated to yield the expected number of pulses arriving 5ps from the mean.

$$\frac{1,000}{\sqrt{2\pi}} \int_5^{\infty} \exp\left(-\frac{1}{2} \frac{x^2}{10^2}\right) dx \quad (13)$$

As in the 2.3.1, this integral cannot be evaluated numerically using the current limits, and instead the limits of (5, 10) are applied.

The expected amount of pulses arriving 5ps after the mean is 1,490

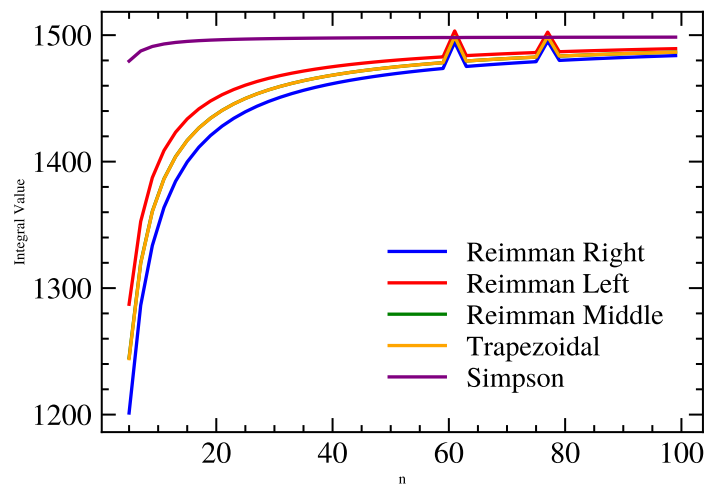


Figure 8: Value of integral for various number of points used in integral calculation, an unexplained bumps in the value occurs for all methods when specific numbers of points are used with the exception of the Simpson method.